



Cite this: *Phys. Chem. Chem. Phys.*,
2016, 18, 21412

Planar $B_3S_2H_3^-$ and $B_3S_2H_3$ clusters with a five-membered B_3S_2 ring: boron–sulfur hydride analogues of cyclopentadiene†

Da-Zhi Li,^{*a} Rui Li,^b Li-Juan Zhang,^a Ting Ou^b and Hua-Jin Zhai^{*bc}

Boron clusters can serve as inorganic analogues of hydrocarbons or polycyclic aromatic hydrocarbons (PAHs). We present herein, based upon global searches and electronic structural calculations at the B3LYP and CCSD(T) levels, the global-minimum structures of two boron–sulfur hydride clusters: $C_{2v} B_3S_2H_3^-$ (**1**, 2B_1) and $C_{2v} B_3S_2H_3$ (**2**, 1A_1). Both species are perfectly planar and feature a five-membered B_3S_2 ring as the structural core, with three H atoms attached terminally to the B sites. Chemical bonding analysis shows that $C_{2v} B_3S_2H_3^-$ (**1**) has a delocalized 5π system within a heteroatomic B_3S_2 ring, analogous to the π bonding in cyclopentadiene, $D_{5h} C_5H_5$. The corresponding closed-shell $C_{2v} B_3S_2H_3^{2-}$ (**3**, 1A_1) dianion is only a local minimum. At the single-point CCSD(T) level, it is 5.7 kcal mol⁻¹ above the chain-like C_1 (1A) open structure. This situation is in contrast to the cyclopentadienyl anion, $C_5H_5^-$, a prototypical aromatic hydrocarbon with a π sextet. The $C_{2v} B_3S_2H_3$ (**2**) neutral cluster is readily obtained upon removal of one π electron from $C_{2v} B_3S_2H_3^-$ (**1**). The anion photoelectron spectrum of $C_{2v} B_3S_2H_3^-$ (**1**) and the infrared absorption spectrum of $C_{2v} B_3S_2H_3$ (**2**) are predicted. The $C_{2v} B_3S_2H_3^-$ (**1**) species can be stabilized in sandwich-type $C_{2h} [(B_3S_2H_3)_2Fe]^{2-}$ and salt $C_{2h} [(B_3S_2H_3)_2Fe]Li_2$ complexes. An intriguing difference is observed between the pattern of π sextet in $C_{2v} B_3S_2H_3^{2-}$ (**3**) dianion and that in cyclopentadienyl anion. The present work also sheds light on the mechanism of structural evolution in the $B_3S_2H_3^{0/-1/2-}$ series with charge states.

Received 7th June 2016,
Accepted 24th June 2016

DOI: 10.1039/c6cp03952a

www.rsc.org/pccp

1. Introduction

Boron is known for its rich chemistry, which is probably only second to carbon. This is entirely due to the fact that boron is an electron-deficient element. Boron-based nanoclusters^{1–20} have recently attracted widespread attention in chemistry and materials science, unraveling intriguing structural and chemical bonding properties. In particular, it is firmly established that there exists an analogous relationship between boron-based clusters and planar hydrocarbons, the latter including polycyclic aromatic hydrocarbons (PAHs). For example, the planar $D_{3h} B_{12}H_6$ cluster

was shown to be a boron hydride analogue of benzene,⁹ the planar concentric π aromatic $D_{6h} B_{18}H_6^{2+}$ (the so-called borannulenes) turned out to be analogous to [10]annulene, $D_{10h} C_{10}H_{10}$,^{5a} and the planar $C_{3h} B_6H_3^+$,^{5b} $D_{2h} B_4H_2$, $C_{2h} B_8H_2$, and $C_{2h} B_{12}H_2$ clusters^{6a} were revealed to be inorganic analogues of the cyclopropene cation $D_{3h} C_3H_3^+$, ethylene $D_{2h} C_2H_4$, 1,3-butadiene $C_{2h} C_4H_6$, and 1,3,5-hexatriene $C_{2h} C_6H_8$, respectively. In terms of the bonding nature, boron hydride clusters are found to possess aromaticity and antiaromaticity according to the Hückel rules, akin to hydrocarbons.

Bonding analogy also exists between boron oxides, boron sulfides, boron–nitrogen hydrides, boron–oxygen hydrides, boron–sulfur hydrides, and hydrocarbons.^{8,10–20} For binary B–O clusters, their isovalent B–S clusters and ternary B–X–H (X = O, S, or N) clusters, the B–X heteroatomic rings appear to be crucial structural blocks. Among the species with a heterocyclic B–X six-membered ring are $B_3O_3H_3$ and $B_3N_3H_6$,^{12–18} which possess a hexagonal B_3X_3 (X = O or N) ring as the core. These are considered as analogues of benzene, owing to the delocalized π sextet in the B_3X_3 ring. An inorganic analogue of benzene can also be made solely using B and O atoms. Indeed, a $D_{3h} B_6O_6$ cluster,² named boronyl boroxine, was shown to be an inorganic benzene or boroxine ($D_{3h} B_3O_3H_3$). Boronyl boroxine

^a Binzhou Key Laboratory of Materials Chemistry, Department of Chemical Engineering, Binzhou University, Binzhou 256603, China.
E-mail: ldz005@126.com

^b Nanocluster Laboratory, Institute of Molecular Science, Shanxi University, Taiyuan 030006, China. E-mail: hj.zhai@sxu.edu.cn

^c State Key Laboratory of Quantum Optics and Quantum Optics Devices, Shanxi University, Taiyuan 030006, China

† Electronic supplementary information (ESI) available: Alternative optimized low-lying structures of $B_3S_2H_3$, $B_3S_2H_3^-$, and $B_3S_2H_3^{2-}$, along with their relative energies at the B3LYP/aug-cc-pVTZ and single-point CCSD(T)//B3LYP/aug-cc-pVTZ levels (Fig. S1–S3) and the adaptive natural density partitioning (AdNDP) bonding pattern of the chain-like structure of the $B_3S_2H_3^{2-}$ dianion (Fig. S4). See DOI: 10.1039/c6cp03952a

is readily formulated as $B_3O_3(BO)_3$, in which three boronyl (BO) groups¹ substitute the H terminals in $B_3O_3H_3$. Similar to benzene, D_{3h} $B_3O_3X_3$ ($X = BO, H$) were explored as ligands to form transition metal complexes, such as sandwich-type D_{3d} $(B_3O_3X_3)_2Cr$,² D_{3d} $(B_3O_3X_3)_2V$,^{3a} and perfectly planar $(B_3O_3H_3)_nM^+$ ($n = 1, 2; M = Cu, Ag, Au$) complexes.^{3b}

Stable boron-containing compound clusters can also possess a rhombic B_2X_2 ($X = O, S, N$) structural core, such as in C_{2v} $B_2N_2H_4$,^{19,20} C_{2v} $B_2S_2H_2$ and $B_2O_2H_2$,¹¹ C_{2v} B_5O^- ,^{8e} and C_{2v} B_4S_4 .¹⁰ Bonding analyses revealed a four-center four-electron (4c-4e) π bond, that is, the so-called o-bond, in these clusters. The o-bond clusters are 4π systems in a nonbonding/bonding combination, which is in contrast to the antibonding/bonding combination in the classical 4π antiaromatic cyclobutadiene (C_4H_4).

Between the six-membered B–X ring systems and the rhombic ones, heteroatomic five-membered B–X rings are anticipated to be present. However, such species have remained scarce in the literature. Very recently, a planar closed-shell D_{2h} $B_6S_6^{2-}$ cluster with twin B_3S_2 five-membered rings was characterized computationally.⁶ Bonding analyses showed that D_{2h} $B_6S_6^{2-}$ possesses 10 delocalized π electrons, closely analogous to the bonding pattern of naphthalene ($C_{10}H_8$). The study also suggested that boron sulfide clusters appear to favor five-membered B_3S_2 ring structures, in contrast to the boron oxides that feature a hexagonal B_3O_3 ring.² Now that the D_{2h} $B_6S_6^{2-}$ cluster with twin B_3S_2 rings has been established as a boron sulfide analogue of naphthalene, can we push further along this line to design boron sulfide clusters with an isolated B_3S_2 five-membered ring? Can these species be inorganic analogues of cyclopentadiene (D_{5h} C_5H_5), or cyclopentadienyl anion (D_{5h} $C_5H_5^-$)? The simplest candidates for such designer species should be $B_3S_2H_3^{0/-/2-}$ clusters, which are chosen as targets for the present study.

In this contribution, we report a systematic computational study on the structural and electronic properties and chemical bonding of ternary $B_3S_2H_3^{0/-/2-}$ clusters. The computations involve global-minimum searches, electronic structural calculations at the density-functional theory (DFT) and coupled-cluster theory (CCSD(T)) levels, and bonding and aromaticity analyses. The global-minimum structures, C_{2v} $B_3S_2H_3^-$ (**1**) and C_{2v} $B_3S_2H_3$ (**2**), are perfectly planar, each featuring a five-membered B_3S_2 heteroatomic ring. A proposal is put forward that C_{2v} $B_3S_2H_3^-$ (**1**) is an inorganic analogue of cyclopentadiene. The corresponding C_{2v} $B_3S_2H_3^{2-}$ (**3**) dianion is analogous to the cyclopentadienyl anion, albeit the former is only a local minimum on the potential energy surface, which is probably due to intramolecular Coulomb repulsion in the dianion. Canonical molecular orbital (CMO) and adaptive natural density partitioning (AdNDP)²¹ analyses reveal that the three delocalized π CMOs in C_{2v} $B_3S_2H_3^-$ (**1**) and $B_3S_2H_3^{2-}$ (**3**) show one to one correspondence to those in cyclopentadiene and the cyclopentadienyl anion, respectively. This work suggests that a variety of boron–sulfur hydride clusters may be designed on the basis of the analogy to hydrocarbons or PAHs. Inspired by the fact that cyclopentadiene is a ligand in the celebrated sandwich-type ferrocene, $(C_5H_5)_2Fe$, we further explore the viability of C_{2v} $B_3S_2H_3^-$ (**1**) cluster as potential ligands for coordination compounds. In parallel with

$(C_5H_5)_2Fe$ complexes (**4** and **5**), a series of sandwich-type transition metal complexes, C_{2h} $[(B_3S_2H_3)_2Fe]^{2-}$ (**6**), C_{2v} $[(B_3S_2H_3)_2Fe]^{2-}$ (**7**), C_{2h} $[(B_3S_2H_3)_2Fe]Li_2$ (**8**), and C_{2v} $[(B_3S_2H_3)_2Fe]Li_2$ (**9**), are calculated. In the dianionic complexes (**6** and **7**), two $B_3S_2H_3^-$ (**1**) clusters are stabilized by a Fe atom and their structural and chemical integrity are well maintained. Notably, the complexes (**6** and **7**) can be further stabilized by two Li^+ counter-cations in **8** and **9**.

2. Computational methods

Global-minimum searches for the $B_3S_2H_3^{0/-/2-}$ systems were conducted using the Gradient Embedded Genetic Algorithm (GEGA)^{22,23} and Coalescence Kick (CK)^{24,25} programs, aided by manual structural constructions. Specifically, a total of 5000 structures were probed for the $B_3S_2H_3^-$ monoanion cluster using the CK method, which was complemented by GEGA searches. Structures for the $B_3S_2H_3$ neutral and the $B_3S_2H_3^{2-}$ dianion were computed primarily based on the low-lying structures of $B_3S_2H_3^-$. Considering the connections between the potential energy surfaces of $B_3S_2H_3^{0/-/2-}$, additional computer searches for $B_3S_2H_3$ and $B_3S_2H_3^{2-}$ do not seem necessary.

Full structural optimizations and frequency calculations were subsequently carried out for the low-lying isomeric $B_3S_2H_3^{0/-/2-}$ structures using the hybrid B3LYP method^{26,27} with the basis set of aug-cc-pVTZ, as implemented in the Gaussian 09 software package.²⁸ For the sandwich complexes, the Stuttgart relativistic small core basis set and effective core potential (Stuttgart RSC 1997 ECP)²⁹ were employed for Fe. Structural optimizations were performed for these complexes by taking into consideration different spin-multiplicity states. Furthermore, relative energies for the low-lying isomers of $B_3S_2H_3^{0/-/2-}$ were refined using single-point CCSD(T) calculations^{30–32} at the B3LYP geometries. AdNDP²¹ and CMO analyses, as well as nucleus-independent chemical shift (NICS)³³ calculations, were carried out to elucidate the nature of bonding and aromaticity in $B_3S_2H_3^{0/-/2-}$. The NBO 5.0 program³⁴ was used to calculate the natural atomic charges.

3. Results and discussion

3.1. Perfectly planar C_{2v} $B_3S_2H_3^{-0/2-}$ clusters with a heteroatomic five-membered B_3S_2 ring

The global-minimum structure of the $B_3S_2H_3^-$ monoanion is **1** (C_{2v} , 2B_1), as illustrated in Fig. 1 along with that of $B_3S_2H_3$ **2** (C_{2v} , 1A_1). Also shown is a relevant structure **3** (C_{2v} , 1A_1) of the $B_3S_2H_3^{2-}$ dianion, which represents a low-lying local minimum. Selected alternative optimized structures of $B_3S_2H_3^{-0/2-}$ are presented in Fig. S1–S3 in the ESI† The global minimum $B_3S_2H_3^-$ (**1**, 2B_1) is perfectly planar with C_{2v} symmetry, which lies 13.45 and 11.47 kcal mol⁻¹ lower than the second lowest-lying isomer, $B_3S_2H_3^-$ (C_s , $^2A'$), at B3LYP and single-point CCSD(T) levels, respectively (Fig. S1, ESI†). The observation indicates that the $B_3S_2H_3^-$ monoanion has a well-defined, cyclic global-minimum. $B_3S_2H_3^-$ (**1**) can be constructed by connecting three H terminals to a heteroatomic B_3S_2 five-membered ring, which is similar to

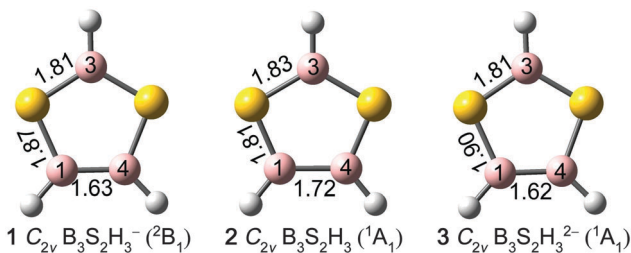


Fig. 1 Global-minimum structures of $C_{2v} B_3S_2H_3^-$ (**1**, 2B_1) and $C_{2v} B_3S_2H_3$ (**2**, 1A_1) at the B3LYP/aug-cc-pVTZ level, along with a local minimum of $C_{2v} B_3S_2H_3^{2-}$ (**3**, 1A_1). All three structures possess a heteroatomic B_3S_2 five-membered ring. Selected bond distances are labeled in angstroms. The B atom is in pink, S in yellow, and H in gray.

the situation of $C_{2v} B_2S_2H_2$.¹¹ The latter species is viewed as two H terminals attached to a rhombic B_2S_2 ring.

The latest recommended covalent radii give the upper bounds of single B–B, double B=B, and triple B≡B bonds as 1.70, 1.56, and 1.46 Å, respectively.³⁵ The B–B distance in **1** is 1.63 Å, which is somewhat shorter than a typical B–B single bond. The B–S distances are slightly uneven (1.81 *versus* 1.87 Å), hinting at possible repulsive interaction between the top and bottom portions of the B_3S_2 ring.

The $B_3S_2H_3$ (**2**, 1A_1) cluster represents the neutral global minimum. It may be reached from $B_3S_2H_3^-$ (**1**) by removing one valence electron from its highest occupied molecular orbital (HOMO), which is singly occupied. Structure **2** is also perfectly planar with a five-membered B_3S_2 ring, which is ~ 8 kcal mol⁻¹ lower in energy than its nearest competitive isomer (Fig. S2, ESI†). The B–B distance in **2** is 1.72 Å, comparable to a typical B–B single bond.³⁵ The B–S bonds appear to be relatively even, 1.81 *versus* 1.83 Å. Nonetheless, the B–S bonds in **1** and **2** should be roughly viewed as, or slightly stronger than single bonds, which are comparable to those in the B_3S_2 core of the $D_{2h} B_6S_6^-$ cluster.⁶

It is straightforward to locate a dianion cluster, $C_{2v} B_3S_2H_3^{2-}$ (**3**, 1A_1) (Fig. 1), by adding one electron to the singly-occupied HOMO of $B_3S_2H_3^-$ (**1**). Structure **3** is a closed-shell cluster, which is also perfectly planar and represents a true minimum on the potential energy surface. However, our GEGA and CK structural searches show that **3** is only a low-lying isomer for the dianion system (Fig. S3, ESI†). A chain-like open structure, C_s (1A), turns out to be 11.97 and 5.67 kcal mol⁻¹ below structure **3** at B3LYP and CCSD(T) levels, respectively. The chain-like C_1 (1A) dianion structure is in stark contrast to the ring-like structures **2**, **1**, and **3**. It is composed of the BSH and B(BS)H₂ units, in which a BS group serves as a terminal ligand, similar to the $B_6S_6^{0/-/2-}$ clusters.⁶ Chemical bonding in this chain-like structure appears to be classical; see below for details. We stress that for a dianion system such as $B_3S_2H_3^{2-}$, the energetics of the isomeric structures is generally considered to be less reliable by the state-of-the-art quantum chemistry. Thus, the triplet structures of $B_3S_2H_3^{2-}$, which actually become competitive in this charge state, are not discussed here. Indeed, the $B_3S_2H_3^{2-}$ dianion is intrinsically unstable against electron autodetachment and it does not seem meaningful to discuss

Table 1 Calculated natural charges (q , in $|e|$) of $C_{2v} B_3S_2H_3^{2-}$ (**3**), $C_{2v} B_3S_2H_3^-$ (**1**), and $C_{2v} B_3S_2H_3$ (**2**) at the B3LYP/aug-cc-pVTZ level

Species	B1 ^a	B3 ^a	S
$C_{2v} B_3S_2H_3^{2-}$ (3)	-0.468	-0.283	-0.254
$C_{2v} B_3S_2H_3^-$ (1)	-0.169	-0.018	-0.205
$C_{2v} B_3S_2H_3$ (2)	+0.103	+0.191	-0.117

^a The B atoms are labeled as shown in Fig. 1.

the bare dianion species, except for the nature of bonding. Only the relevant salt complexes with counter-ions are thermodynamically stable.

For the ring-like $B_3S_2H_3^{0/-/2-}$ (**2**, **1**, and **3**) series, the B–B distance shrinks (1.72 → 1.63 → 1.62 Å) upon addition of extra electrons, indicating that the charges in the anion and dianion are significantly involved in B–B bonding, which is fully supported by the calculated natural charges (Table 1). Specifically, the B1/B4 and B3 centers in **2** are slightly, positively charged by +0.10/+0.10 and +0.19 $|e|$, respectively. For the first charge, these centers gain the extra charge of 0.27/0.27 and 0.21 $|e|$ in **1**. For the second charge, the B centers further gain the charge of 0.30/0.30 and 0.26 $|e|$ in **3**. In other words, 75% and 86% of the first and second charges in **1/3** go to the B centers, respectively. In the meantime, the B–S distances become increasingly uneven: 1.83/1.81 Å in **2**, 1.81/1.87 Å in **1**, and 1.81/1.90 Å in **3**. This observation suggests that the charges in **1** and **3** also induce repulsive interactions within the B_3S_2 ring.

3.2. The $C_{2v} B_3S_2H_3^-$ (**1**) cluster as an inorganic analogue of cyclopentadiene

The structural searches support our initial idea that a five-membered, heteroatomic B_3S_2 ring can serve as a robust structural core in boron–sulfur hydride clusters. The $C_{2v} B_3S_2H_3^-$ (**1**, 2B_1) and $B_3S_2H_3$ (**2**, 1A_1) clusters are the global minima on their potential energy surfaces, whereas $C_{2v} B_3S_2H_3^{2-}$ (**3**, 1A_1) also represents a true minimum. Since the $B_6S_6^{0/-/2-}$ clusters with fused twin B_3S_2 rings were recently shown to be analogous to naphthalene,⁶ it is natural to speculate that the present $B_3S_2H_3^{0/-/2-}$ (**1–3**) species with an isolated B_3S_2 ring should be boron–sulfur hydride analogues of cyclopentadiene or cyclopentadienyl anion. To be precise, the open-shell $B_3S_2H_3^-$ (**1**) anion is anticipated to be analogous to cyclopentadiene, whereas the closed-shell $B_3S_2H_3^{2-}$ (**3**) dianion is an analogue of the cyclopentadienyl anion.

To confirm the speculation, we choose to analyze the bonding in $B_3S_2H_3^{2-}$ (**3**) using AdNDP,²¹ because this analysis is currently applicable only for closed-shell species. As an extension of natural bond orbital (NBO) analysis, AdNDP represents the electronic structure of a molecular system in terms of n -center two-electron ($nc-2e$) bonds, where the values of n range from one to the total number of atoms in the system. AdNDP thus recovers not only the classical Lewis bonding elements (lone-pairs and $2c-2e$ bonds), but also the delocalized $nc-2e$ bonds.

As illustrated in Fig. 2, the $B_3S_2H_3^{2-}$ (**3**) dianion has a π sextet, whose three delocalized CMOs exhibit one-to-one correspondence to those of cyclopentadienyl anion. The AdNDP scheme of

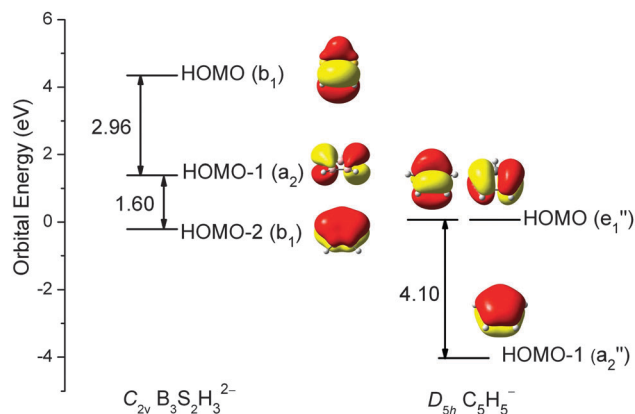


Fig. 2 Energy levels of the canonical molecular orbitals (CMOs) for the π sextets in $C_{2v} B_3S_2H_3^{2-}$ and $D_{5h} C_5H_5^-$ at the B3LYP/aug-cc-pVTZ level.

$B_3S_2H_3^{2-}$ (**3**) (Fig. 3) appears to be simple. It possesses 26 valence electrons, featuring four B–S and one B–B 2c-2e σ bonds within the B_3S_2 ring, three terminal 2c-2e B–H σ bonds, and two S 3s lone-pairs. The remaining three AdNDP elements are delocalized 5c-2e π bonds (Fig. 3, second row), which make **3** an inorganic analogue of the cyclopentadienyl anion. The $C_{2v} B_3S_2H_3^-$ (**1**, 2B_1) monoanion can be obtained by removing one electron from **3**. It is easy to know that **1** has 5 π electrons, analogous to cyclopentadiene, $D_{5h} C_5H_5$. To our knowledge, $B_3S_2H_3^-$ (**1**) is the first heteroatomic, inorganic analogue of cyclopentadiene ever reported in the literature.

NICS calculations also support the above idea (Table 2). Calculated at the center of the B_3S_2 ring and at 1 Å above the center, the NICS(0), NICS(1), and NICS_{zz}(1) values of $C_{2v} B_3S_2H_3^{2-}$ (**3**) at the B3LYP/aug-cc-pVTZ level are –5.27, –5.06, and –13.64 ppm, respectively, which are nearly identical to those of the naphthalene analogue, $D_{2h} B_6S_6^-$; NICS(0) = –5.0 ppm, NICS_{zz}(1) = –13.7 ppm.⁶ The corresponding values for the cyclopentadienyl anion are –12.29,

Table 2 Calculated nucleus-independent chemical shift (NICS) and NICS_{zz} values of $C_{2v} B_3S_2H_3^{2-}$ (**3**) at the B3LYP/aug-cc-pVTZ level, as compared to those of the corresponding hydrocarbon, $D_{5h} C_5H_5^-$

Species	NICS(0) ^a	NICS(1) ^a	NICS _{zz} (1) ^a
$C_{2v} B_3S_2H_3^{2-}$ (3 , 1A_1)	–5.27	–5.06	–13.64
$D_{5h} C_5H_5^-$ ($^1A_1'$)	–12.29	–9.66	–34.54

^a NICS(0) and NICS(1) values are calculated at the ring center and 1 Å above it, respectively.

–9.66, and –34.34 ppm. These NICS values indicate that $C_{2v} B_3S_2H_3^{2-}$ (**3**) and $D_{5h} C_5H_5^-$ are aromatic systems, further confirming their chemical analogy.

It is interesting to note that, despite the analogy, the π sextet in $B_3S_2H_3^{2-}$ (**3**) differs markedly from that in $D_{5h} C_5H_5^-$ (Fig. 2) in terms of the energetics of π CMOs. For the π sextet in $D_{5h} C_5H_5^-$, the upper two CMOs, that is, the HOMO (e_1'') orbitals, are doubly degenerate and situated significantly above the completely bonding CMO, HOMO–1 (a_2''), by 4.10 eV. However, for $B_3S_2H_3^{2-}$ (**3**), the five B/S centers are not equivalent. As a consequence, the partially bonding/antibonding CMOs (HOMO and HOMO–1) are no longer degenerate, rather they split in energy by as much as 2.96 eV. Furthermore, the energy gap between the completely bonding CMO (HOMO–2) and the partially bonding/antibonding CMOs is reduced (to 1.60 eV), whereas the splitting within the latter surpasses the energy gap. The underlying mechanism is that, for the partially bonding/antibonding pair of CMOs in **3**, the HOMO is largely boron-based and high in energy with respect to HOMO–1, which is S 3p based. The two CMOs cannot be made close in energy despite the mixing of the five centers in the ring. One advantage of this unique π scheme in **3** is that the system no longer needs to possess exactly six electrons in order to be stable, making $B_3S_2H_3^-$ (**1**) and $B_3S_2H_3$ (**2**) relatively stable and suitable for forming transition metal sandwich complexes, as discussed below.

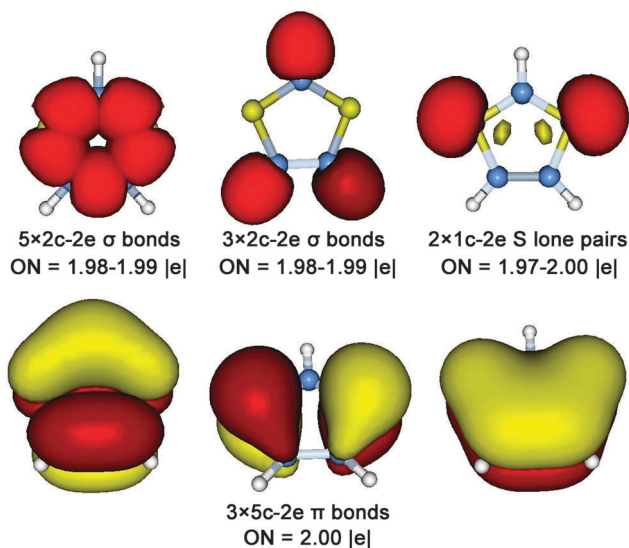


Fig. 3 The bonding pattern of $C_{2v} B_3S_2H_3^{2-}$ based on adaptive natural density partitioning (AdNDP) analysis. Occupation numbers (ONs) are shown.

3.3. Predicted electronic and vibrational properties of $C_{2v} B_3S_2H_3^-$ (**1**) and $C_{2v} B_3S_2H_3$ (**2**)

To aid future experimental characterization of $C_{2v} B_3S_2H_3^-$ (**1**, 2B_1) and $C_{2v} B_3S_2H_3$ (**2**, 1A_1) clusters as the global-minimum structures, we report their calculated electronic and vibrational properties, which are measurable using the popular gas-phase techniques of anion photoelectron spectroscopy (PES) and infrared (IR) spectroscopy, respectively. Anion PES measures the adiabatic and vertical detachment energies (ADE and VDE) of an anion species and access the electronic ground state and excited states of the corresponding neutral cluster, whereas IR spectroscopy readily obtains the characteristic vibrational signatures of a neutral cluster. The calculated ground-state ADE and VDE of $B_3S_2H_3^-$ (**1**) are 1.90 and 2.05 eV, respectively, at the B3LYP/aug-cc-pVTZ level. These values are refined to 1.81 and 1.98 eV at the single-point CCSD(T) level.

The simulated PES spectrum of $B_3S_2H_3^-$ (**1**) is presented in Fig. 4, which is based on computational VDE data at the B3LYP/aug-cc-pVTZ and time-dependent B3LYP (TD-B3LYP)^{36,37} levels. The first 13 electron detachment channels are calculated with

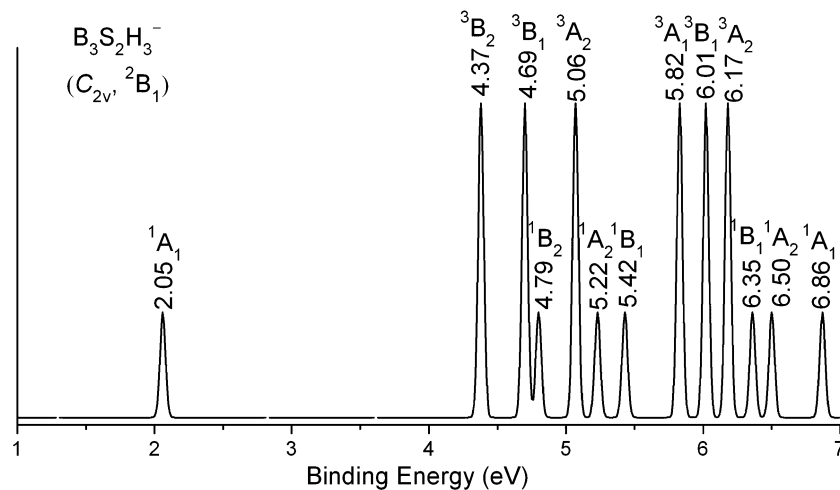


Fig. 4 Simulated photoelectron spectrum of the C_{2v} $B_3S_2H_3^-$ ($1, {}^2B_1$) anion at the B3LYP/aug-cc-pVTZ level. The simulations were done by fitting the distribution of the calculated vertical detachment energies (VDEs) with unit-area Gaussian functions of 0.04 eV half-width.

Table 3 Calculated lowest vibrational frequencies (ν_{\min} , in cm^{-1}), vertical ionization potentials (VIPs, in eV), and formation energies (FEs, in kcal mol^{-1}) of C_{2v} $B_3S_2H_3^-$ (**1**), C_{2v} $B_3S_2H_3$ (**2**), and their relevant sandwich-type complexes (**6–9**). For comparison, those of the cyclopentadiene counterparts, D_{5d} $(C_5H_5)_2Fe$ (**4**) and D_{5h} $(C_5H_5)_2Fe$ (**5**), have also been tabulated

Species	ν_{\min}	VIP	FE ^a
C_{2v} $B_3S_2H_3^-$ (1)	275.72	2.05	
C_{2v} $B_3S_2H_3$ (2)	161.72	10.02	
D_{5d} $(C_5H_5)_2Fe$ (4)	-40.37	7.05	-192.17
D_{5h} $(C_5H_5)_2Fe$ (5)	31.97	7.06	-192.56
C_{2h} $[(B_3S_2H_3)_2Fe]^{2-}$ (6)	25.08		-4.71 ^b
C_{2v} $[(B_3S_2H_3)_2Fe]^{2-}$ (7)	18.94		-3.63 ^b
C_{2h} $[(B_3S_2H_3)_2Fe]Li_2$ (8)	23.49	6.84	-87.60 ^b
C_{2v} $[(B_3S_2H_3)_2Fe]Li_2$ (9)	25.20	5.70	-87.36 ^b

^a In the FE calculations, free energy corrections are included. ^b The difference in FE between **6** and **8**, as well as between **7** and **9**, is attributed to the intramolecular Coulomb repulsion in **6** and **7** due to the multiple charges.

VDE values from 2.05 to 6.86 eV. The spectral pattern features an energy gap of ~ 2.3 eV, suggesting that the corresponding neutral species, $B_3S_2H_3$ (**2**), is electronically quite stable and chemically inert, in line with the π bonding pattern presented in Fig. 2. Note that all electronic states in Fig. 4 are the ground state and excited states of the $B_3S_2H_3$ (**2**) neutral cluster.

Furthermore, the vertical ionization potential (VIP) of C_{2v} $B_3S_2H_3$ (**2**, 1A_1) is predicted to be 10.02 eV at the B3LYP/aug-cc-pVTZ level (Table 3). As for the IR spectrum, the simulation of $B_3S_2H_3$ (**2**) is presented in Fig. 5. Three adjacent peaks are revealed at 2640–2680 cm^{-1} , which correspond to B–H symmetric stretchings. Among them, the intense peak at 2661 cm^{-1} (a_1) is associated with the B1–H and B4–H symmetric stretching. Other two intense peaks at 1108 cm^{-1} (b_2) and 655 cm^{-1} (a_1) are due to B–H rocking vibration and B–B stretching, respectively.

3.4. On the chain-like structure of $B_3S_2H_3^{2-}$ (C_1 , 1A) and the structural evolution in the $B_3S_2H_3^{0/-/2-}$ series

While ring-like structures **1–3** of $B_3S_2H_3^{0/-/2-}$ (Fig. 1) are the focus of this study, the lowest-energy, chain-like open structure

C_1 (1A) (Fig. S3, ESI[†]) of the $B_3S_2H_3^{2-}$ dianion requires special attention. Fig. 6 shows the optimized C_1 (1A) structure at the B3LYP level along with bond distances, its Lewis structure as well as that of $B_3S_2H_3^{0/-/2-}$ (**3**), and its HOMO. Based on the bond distances, the B–H (1.23–1.24 Å) and B–B (1.63 and 1.75 Å) bonds are assigned to single bonds.³⁵ The elongation of the latter B–B bond may be partially attributed to the Coulomb repulsion in the dianion system. Orbital component analysis of the HOMO (Fig. 6(d)) shows 12% and 11% of B 2p from the top two B atoms on the left side and 74% S 3p from the S atom on the right side, and the overall nature of the HOMO is antibonding. The short and long B–S distances are assigned to triple B \equiv S and double B=S bonds, respectively. The above assignments offer a classical Lewis structure as shown in Fig. 6(b), which can be further confirmed from the AdNDP analysis (Fig. S4, ESI[†]). The Lewis structure differs markedly from the delocalized π sextet in $B_3S_2H_3^{2-}$ (**3**) (Fig. 1 and 6(c)).

Qualitatively, the chain-like open structure of $B_3S_2H_3^{2-}$ may be understood as follows. Going from $B_3S_2H_3^-$ (**1**) to $B_3S_2H_3^{2-}$ (**3**), an increase of natural charge occurs on the B atoms, particularly B1 and B4 (Table 1), which gives B1/B4 centers the potential to become sp^3 hybridized. Indeed, from **1** to **3** about 60% of the extra charge is accumulated on the B1–B4 edge of the ring and the B1/B4 centers in **3** can be roughly viewed as B^- . For such B centers, tetracoordination is a favorable configuration, justifying the chain-like open structure (Fig. 6(a)). In addition, the chain-like structure of $B_3S_2H_3^{2-}$ also facilitates the release of Coulomb repulsion between the two charges.

The evolution of ring-like *versus* chain-like structures in $B_3S_2H_3^{0/-/2-}$ with charge states is summarized in Fig. 7. A chain-like open structure can also be traced for the neutral system, albeit with a substantial structural reorganization. It is the eighth structure in Fig. S2 (ESI[†]), which is 18.35 kcal mol^{-1} above global minimum **2** at the B3LYP level. From neutral to the monoanion, the relative energy of two isomers changes only slightly. However, from the monoanion to the dianion, the energy order reverses. The ring-like structure for the monoanion is the global minimum (**1**),

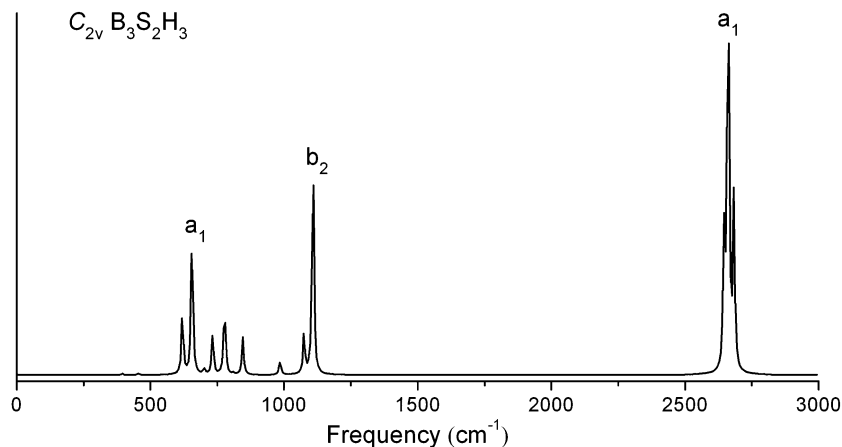


Fig. 5 Simulated infrared (IR) spectrum of the C_{2v} $B_3S_2H_3$ (**2**, 1A_1) neutral cluster.

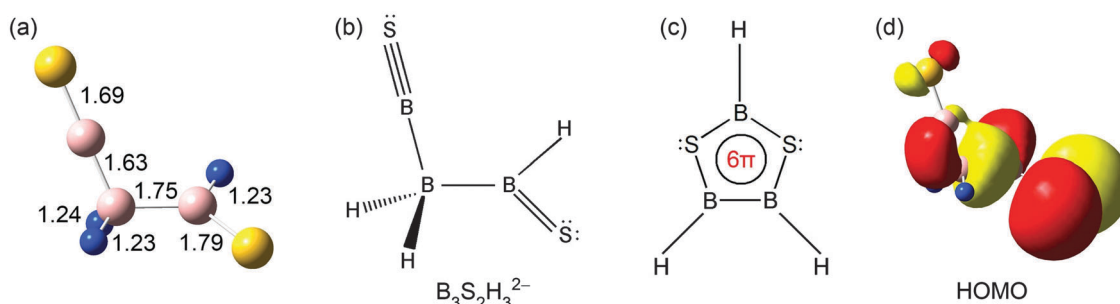


Fig. 6 Structure and bonding of the chain-like $B_3S_2H_3^{2-}$. (a) Optimized C_1 (1A) structure at the B3LYP/aug-cc-pVTZ level. (b) Lewis presentation. (c) Lewis presentation of the ring-like structure of C_{2v} $B_3S_2H_3^{2-}$ (**3**, 1A_1). (d) Picture of the HOMO orbital of $B_3S_2H_3^{2-}$ C_1 (1A).

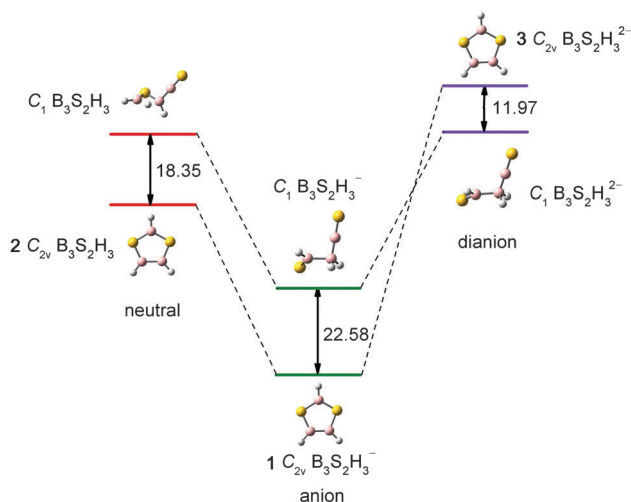


Fig. 7 Schematic diagram for the energetics of two isomeric structures (ring-like versus chain-like) in three charge states. The relative energies (in kcal mol^{-1}) are shown at the B3LYP/aug-cc-pVTZ level.

which is $22.58 \text{ kcal mol}^{-1}$ lower than the chain-like one, whereas the former becomes a high energy isomer for the dianion (**3**). Note that the anion and the dianion differ solely in the number of occupied electrons in the HOMO (one in the anion versus two in the dianion). Based on this fact, the reverse

of energy order for the two isomers should be primarily attributed to intramolecular Coulomb repulsion in the systems. Indeed, the magnitude of Coulomb repulsion is anticipated to be greater for the ring-like **3** than the chain-like isomer. The repulsion is also clearly reflected in B–S distances in the $B_3S_2H_3^{0/-/2-}$ series (Fig. 1), where the B1–S and B4–S distances elongate gradually with the extra charges. Using counter-ions, it should be possible to further stabilize the $B_3S_2H_3^{2-}$ (**3**) dianion in salt type complexes.

3.5. The C_{2v} $B_3S_2H_3^-$ (**1**) cluster as a potential ligand in sandwich-type complexes

Since the preparation of ferrocene, D_{5h} $(C_5H_5)_2Fe$, in the early 1950s,³⁸ ferrocene and its derivatives were found to have promising uses in medicine, biology, electrochemistry, catalysis, and many other fields, due to their special sandwich structures and aromaticity.^{39–42} It is thus of interest to pursue sandwich-type transition metal complexes using the present C_{2v} $B_3S_2H_3^-$ (**1**, 2B_1) cluster as a ligand. Fig. 8 shows the optimized structures of C_{2h} $[(B_3S_2H_3)_2Fe]^{2-}$ (**6**), C_{2v} $[(B_3S_2H_3)_2Fe]^{2-}$ (**7**), C_{2h} $[(B_3S_2H_3)_2Fe]Li_2$ (**8**), and C_{2v} $[(B_3S_2H_3)_2Fe]Li_2$ (**9**) at the B3LYP level, which are compared with their cyclopentadiene counterparts: D_{5d} $(C_5H_5)_2Fe$ (**4**) and D_{5h} $(C_5H_5)_2Fe$ (**5**).

In complexes **6** and **7**, one Fe atom is sandwiched between two $B_3S_2H_3^-$ (**1**) ligands from the opposite ends along the

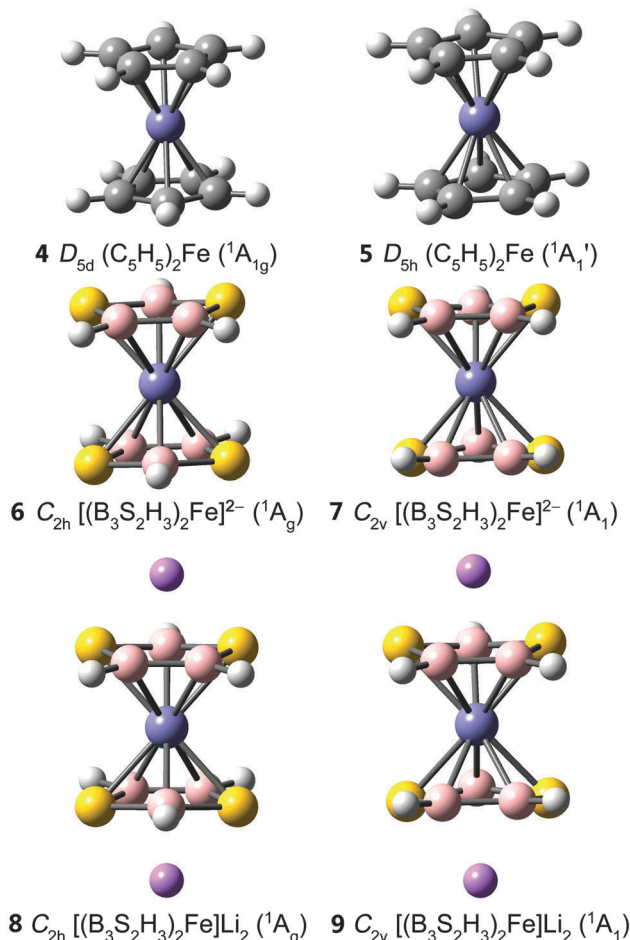


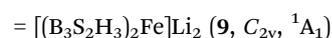
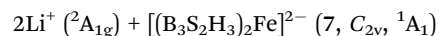
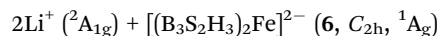
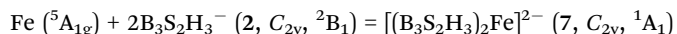
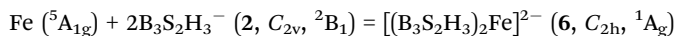
Fig. 8 Sandwich-type complexes C_{2h} [($B_3S_2H_3$)₂Fe]²⁻ (6), C_{2v} [($B_3S_2H_3$)₂Fe]²⁻ (7), C_{2h} [($B_3S_2H_3$)₂Fe]Li₂ (8), and C_{2v} [($B_3S_2H_3$)₂Fe]Li₂ (9) at the B3LYP level, as compared to their cyclopentadiene counterparts, D_{5d} (C_5H_5)₂Fe (4) and D_{5h} (C_5H_5)₂Fe (5). The B atom is in pink, S in yellow, C and H in gray, Fe in blue, and Li in purple.

fivefold axis, forming staggered C_{2h} and eclipsed C_{2v} complexes. Differing from staggered 4 and eclipsed 5, the staggered 6 and eclipsed 7 are both true minima with the lowest vibrational frequency of 25.08 and 18.94 cm^{-1} , respectively (Table 3). Similar to the situation in [$B_3N_3H_6$]₂M,^{43,44} [$B_3O_3X_3$]₂Cr,² [$B_3O_3X_3$]₂V (X = H, BO),^{3a} and [$B_2S_2H_2$]₂Ni,¹¹ the staggered species 6 is more stable with respect to 7. The C_{2h} (6) \rightarrow C_{2v} (7) rotator transition for [($B_3S_2H_3$)₂Fe]²⁻ has a tiny energy barrier of 0.85 $kcal\ mol^{-1}$ at the B3LYP level. Thus C_{2h} [($B_3S_2H_3$)₂Fe]²⁻ (6) and C_{2v} [($B_3S_2H_3$)₂Fe]²⁻ (7) sandwiches may coexist in experiments. These sandwich complexes follow the 18-electron rule, because they are isoivalent to ferrocene.

The structures C_{2h} [($B_3S_2H_3$)₂Fe]Li₂ (8) and C_{2v} [($B_3S_2H_3$)₂Fe]Li₂ (9) are neutral salt complexes. They possess a perfectly planar $B_3S_2H_3$ ⁻ motif, which is obtained when two Li⁺ cations are attached to 6 or 7. Sandwiches 8 and 9 are true minima as well, with the lowest vibrational frequency of 23.49 and 25.20 cm^{-1} , respectively (Table 3). The calculated VIPs of 8 and 9 at the B3LYP level are 6.84 and 5.70 eV, respectively. These values are comparable to and slightly lower than D_{5h} (C_5H_5)₂Fe (5), which has a

calculated VIP of 7.06 eV, suggesting that 8 and 9 are relatively stable neutral species.

To further evaluate the thermodynamic stability of sandwich complexes 6–9, we have calculated their formation energies (FEs) according to the following equations:



In the calculations of FEs, free energy corrections are considered. As shown in Table 3, the FEs are -4.71 , -3.63 , -87.60 , and -87.36 $kcal\ mol^{-1}$ for structures 6–9, respectively. In particular, the FEs for C_{2h} (8) and C_{2v} (9) neutral clusters are substantial, indicating that their formation are highly exothermic and energetically favorable. Note that the calculated FEs of D_{5h} (C_5H_5)₂Fe (5) at the same level is -192.56 $kcal\ mol^{-1}$. Similar to D_{5h} (C_5H_5)₂Fe, η^4 -heterocyclic ($C_2P_2R_2$)₂Ni sandwiches,^{45,46} and metal–benzene complexes $M_n(\text{benzene})_m$ (M = Sc to Cu),⁴⁷ the sandwiches 6–9, especially 8 and 9, may be viable targets for synthetic efforts. The remarkable increase in FE from 6 to 8, as well as from 7 to 9, is primarily ascribed to the intramolecular Coulomb repulsion between the extra charges in 6 and 8.

4. Conclusions

In conclusion, we have studied the smallest boron–sulfur hydride clusters with a heteroatomic, five-membered B–S ring, aiming at the exploration of inorganic analogues of cyclopentadiene or cyclopentadienyl anion. Two boron–sulfur hydride clusters, C_{2v} $B_3S_2H_3^-$ (1) and C_{2v} $B_3S_2H_3$ (2), are shown to possess ring-like global minima with a B_3S_2 core, based upon structural searches and electronic structural calculations at the B3LYP and CCSD(T) levels. Chemical bonding analyses reveal a delocalized 5π system for C_{2v} $B_3S_2H_3^-$ (1), rendering this anion a boron–sulfur hydride analogue of cyclopentadiene. The C_{2v} $B_3S_2H_3$ (2) neutral cluster appears to be electronically robust with a large HOMO–LUMO gap. In contrast, the ring-like C_{2v} $B_3S_2H_3^{2-}$ (3) dianion is only a local minimum, which is slightly higher in energy than the chain-like, open structure, C_1 (1A). Structural evolution of the $B_3S_2H_3^{0/-/2-}$ series with charge states is elucidated. The C_{2v} $B_3S_2H_3^-$ (1) cluster is used as a ligand to design sandwich-type complexes: C_{2h} [($B_3S_2H_3$)₂Fe]²⁻ (6), C_{2v} [($B_3S_2H_3$)₂Fe]²⁻ (7), C_{2h} [($B_3S_2H_3$)₂Fe]Li₂ (8), and C_{2v} [($B_3S_2H_3$)₂Fe]Li₂ (9), akin to ferrocene based on cyclopentadiene as a ligand.

Acknowledgements

This work was supported by the National Natural Science Foundation of China (21573138), the Natural Science Foundation of

Shandong Province (ZR2014BL011), the Research Fund of Binzhou University (2014Y18), and the State Key Laboratory of Quantum Optics and Quantum Optics Devices (KF201402).

References

- (a) H. J. Zhai, Q. Chen, H. Bai, S. D. Li and L. S. Wang, *Acc. Chem. Res.*, 2014, **47**, 2435; (b) H. J. Zhai, S. D. Li and L. S. Wang, *J. Am. Chem. Soc.*, 2007, **129**, 9254; (c) S. D. Li, H. J. Zhai and L. S. Wang, *J. Am. Chem. Soc.*, 2008, **130**, 2573.
- D. Z. Li, H. Bai, Q. Chen, H. G. Lu, H. J. Zhai and S. D. Li, *J. Chem. Phys.*, 2013, **138**, 244304.
- (a) D. Z. Li, S. G. Zhang, J. J. Liu and C. Tang, *Eur. J. Inorg. Chem.*, 2014, 3406; (b) D. Z. Li, C. C. Dong and S. G. Zhang, *J. Mol. Model.*, 2013, **19**, 3219.
- (a) H. J. Zhai, Y. F. Zhao, W. L. Li, Q. Chen, H. Bai, H. S. Hu, Z. A. Piazza, W. J. Tian, H. G. Lu, Y. B. Wu, Y. W. Mu, G. F. Wei, Z. P. Liu, J. Li, S. D. Li and L. S. Wang, *Nat. Chem.*, 2014, **6**, 727; (b) Q. Chen, S. Y. Zhang, H. Bai, W. J. Tian, T. Gao, H. R. Li, C. Q. Miao, Y. W. Mu, H. G. Lu, H. J. Zhai and S. D. Li, *Angew. Chem., Int. Ed.*, 2015, **54**, 8160; (c) H. Bai, Q. Chen, H. J. Zhai and S. D. Li, *Angew. Chem., Int. Ed.*, 2015, **54**, 941; (d) Q. Chen, W. L. Li, Y. F. Zhao, S. Y. Zhang, H. S. Hu, H. Bai, H. R. Li, W. J. Tian, H. G. Lu, H. J. Zhai, S. D. Li, J. Li and L. S. Wang, *ACS Nano*, 2015, **9**, 754; (e) H. J. Zhai, L. S. Wang, A. N. Alexandrova and A. I. Boldyrev, *J. Chem. Phys.*, 2002, **117**, 7917; (f) H. J. Zhai, B. Kiran, J. Li and L. S. Wang, *Nat. Mater.*, 2003, **2**, 827; (g) H. J. Zhai, A. N. Alexandrova, K. A. Birch, A. I. Boldyrev and L. S. Wang, *Angew. Chem., Int. Ed.*, 2003, **42**, 6004; (h) B. Kiran, S. Bulusu, H. J. Zhai, S. Yoo, X. C. Zeng and L. S. Wang, *Proc. Natl. Acad. Sci. U. S. A.*, 2005, **102**, 961; (i) A. P. Sergeeva, D. Yu. Zubarev, H. J. Zhai, A. I. Boldyrev and L. S. Wang, *J. Am. Chem. Soc.*, 2008, **130**, 7244; (j) W. Huang, A. P. Sergeeva, H. J. Zhai, B. B. Averkiev, L. S. Wang and A. I. Boldyrev, *Nat. Chem.*, 2010, **2**, 202; (k) W. L. Li, Q. Chen, W. J. Tian, H. Bai, Y. F. Zhao, H. S. Hu, J. Li, H. J. Zhai, S. D. Li and L. S. Wang, *J. Am. Chem. Soc.*, 2014, **136**, 12257; (l) Y. J. Wang, X. Y. Zhao, Q. Chen, H. J. Zhai and S. D. Li, *Nanoscale*, 2015, **7**, 16054; (m) A. N. Alexandrova, A. I. Boldyrev, H. J. Zhai and L. S. Wang, *Coord. Chem. Rev.*, 2006, **250**, 2811.
- (a) Q. Chen, H. Bai, J. C. Guo, C. Q. Miao and S. D. Li, *Phys. Chem. Chem. Phys.*, 2011, **13**, 20620; (b) D. Z. Li, H. G. Lu and S. D. Li, *J. Mol. Model.*, 2012, **18**, 3161; (c) Q. Chen and S. D. Li, *J. Cluster Sci.*, 2011, **22**, 513.
- (a) D. Z. Li, Q. Chen, Y. B. Wu, H. G. Lu and S. D. Li, *Phys. Chem. Chem. Phys.*, 2012, **14**, 14769; (b) D. Z. Li, H. Bai, T. Ou, Q. Chen, H. J. Zhai and S. D. Li, *J. Chem. Phys.*, 2015, **142**, 014302.
- J. A. Tossell, J. H. Moore, K. McMillan, C. K. Subramaniam and M. A. Coplan, *J. Am. Chem. Soc.*, 1992, **114**, 1114.
- (a) Q. Chen, H. G. Lu, H. J. Zhai and S. D. Li, *Phys. Chem. Chem. Phys.*, 2014, **16**, 7274; (b) J. C. Guo, H. G. Lu, H. J. Zhai and S. D. Li, *J. Phys. Chem. A*, 2013, **117**, 11587; (c) H. J. Zhai, Q. Chen, H. Bai, H. G. Lu, W. L. Li, S. D. Li and L. S. Wang, *J. Chem. Phys.*, 2013, **139**, 174301; (d) T. Ou, W. J. Tian, X. R. You, Y. J. Wang, K. Wang and H. J. Zhai, *Phys. Chem. Chem. Phys.*, 2015, **17**, 29697; (e) W. J. Tian, X. R. You, D. Z. Li, T. Ou, Q. Chen, H. J. Zhai and S. D. Li, *J. Chem. Phys.*, 2015, **143**, 064303; (f) H. J. Zhai, L. M. Wang, S. D. Li and L. S. Wang, *J. Phys. Chem. A*, 2007, **111**, 1030; (g) H. J. Zhai, C. Q. Miao, S. D. Li and L. S. Wang, *J. Phys. Chem. A*, 2010, **114**, 12155; (h) H. J. Zhai, J. C. Guo, S. D. Li and L. S. Wang, *ChemPhysChem*, 2011, **12**, 2549; (i) Q. Chen, H. J. Zhai, S. D. Li and L. S. Wang, *J. Chem. Phys.*, 2012, **137**, 044307; (j) Q. Chen, H. Bai, H. J. Zhai, S. D. Li and L. S. Wang, *J. Chem. Phys.*, 2013, **139**, 044308; (k) H. Bai, H. J. Zhai, S. D. Li and L. S. Wang, *Phys. Chem. Chem. Phys.*, 2013, **15**, 9646; (l) W. J. Tian, H. G. Xu, X. Y. Kong, Q. Chen, W. J. Zheng, H. J. Zhai and S. D. Li, *Phys. Chem. Chem. Phys.*, 2014, **16**, 5129; (m) W. J. Tian, L. J. Zhao, Q. Chen, T. Ou, H. G. Xu, W. J. Zheng, H. J. Zhai and S. D. Li, *J. Chem. Phys.*, 2015, **142**, 134305; (n) L. J. Zhao, W. J. Tian, T. Ou, H. G. Xu, G. Feng, X. L. Xu, H. J. Zhai, S. D. Li and W. J. Zheng, *J. Chem. Phys.*, 2016, **144**, 124301.
- N. G. Szwacki, V. Weber and C. J. Tymczak, *Nanoscale Res. Lett.*, 2009, **4**, 1085.
- D. Z. Li, S. G. Zhang and C. C. Dong, *Eur. J. Inorg. Chem.*, 2016, 1103.
- D. Z. Li, L. J. Zhang, T. Ou, H. X. Zhang, L. Pei, H. J. Zhai and S. D. Li, *Phys. Chem. Chem. Phys.*, 2015, **17**, 16798.
- L. Barton, F. A. Grimm and R. F. Porter, *Inorg. Chem.*, 1966, **5**, 2076.
- W. Harshbarger, G. Lee, R. F. Porter and S. H. Bauer, *Inorg. Chem.*, 1969, **8**, 1683.
- P. W. Fowler and E. Steiner, *J. Phys. Chem. A*, 1997, **101**, 1409.
- J. J. Engelberts, R. W. A. Havenith, J. H. van Lenthe, L. W. Jenneskens and P. W. Fowler, *Inorg. Chem.*, 2005, **44**, 5266.
- C. H. Chang, R. F. Porter and S. H. Bauer, *Inorg. Chem.*, 1969, **8**, 1689.
- J. A. Tossell and P. Lazzarotti, *J. Phys. Chem.*, 1990, **94**, 1723.
- K. L. Bhat, G. D. Markham, J. D. Larkin and C. W. Bock, *J. Phys. Chem. A*, 2011, **115**, 7785.
- (a) N. C. Baird and R. K. Datta, *Inorg. Chem.*, 1972, **11**, 17; (b) N. C. Baird, *Inorg. Chem.*, 1973, **12**, 473.
- A. J. Bridgeman and J. Rothery, *Inorg. Chim. Acta*, 1999, **288**, 17.
- D. Y. Zubarev and A. I. Boldyrev, *Phys. Chem. Chem. Phys.*, 2008, **10**, 5207.
- A. N. Alexandrova, A. I. Boldyrev, Y. J. Fu, X. Yang, X. B. Wang and L. S. Wang, *J. Chem. Phys.*, 2004, **121**, 5709.
- A. N. Alexandrova and A. I. Boldyrev, *J. Chem. Theory Comput.*, 2005, **1**, 566.
- A. P. Sergeeva, B. B. Averkiev, H. J. Zhai, A. I. Boldyrev and L. S. Wang, *J. Chem. Phys.*, 2011, **134**, 224304.
- (a) M. Saunders, *J. Comput. Chem.*, 2004, **25**, 621; (b) P. P. Bera, K. W. Sattelmeyer, M. Saunders, H. F. Schaefer III and P. v. R. Schleyer, *J. Phys. Chem. A*, 2006, **110**, 4287.

- 26 A. D. Becke, *J. Chem. Phys.*, 1993, **98**, 5648.
- 27 C. Lee, W. T. Yang and R. G. Parr, *Phys. Rev. B: Condens. Matter Mater. Phys.*, 1988, **37**, 785.
- 28 M. J. Frisch, G. W. Trucks, H. B. Schlegel, G. E. Scuseria, M. A. Robb, J. R. Cheeseman, G. Scalmani, V. Barone, B. Mennucci, G. A. Petersson, H. Nakatsuji, M. Caricato, X. Li, H. P. Hratchian, A. F. Izmaylov, J. Bloino, G. Zheng, J. L. Sonnenberg, M. Hada, M. Ehara, K. Toyota, R. Fukuda, J. Hasegawa, M. Ishida, T. Nakajima, Y. Honda, O. Kitao, H. Nakai, T. Vreven, J. A. Montgomery, Jr., J. E. Peralta, F. Ogliaro, M. Bearpark, J. J. Heyd, E. Brothers, K. N. Kudin, V. N. Staroverov, R. Kobayashi, J. Normand, K. Raghavachari, A. Rendell, J. C. Burant, S. S. Iyengar, J. Tomasi, M. Cossi, N. Rega, J. M. Millam, M. Klene, J. E. Knox, J. B. Cross, V. Bakken, C. Adamo, J. Jaramillo, R. Gomperts, R. E. Stratmann, O. Yazyev, A. J. Austin, R. Cammi, C. Pomelli, J. W. Ochterski, R. L. Martin, K. Morokuma, V. G. Zakrzewski, G. A. Voth, P. Salvador, J. J. Dannenberg, S. Dapprich, A. D. Daniels, Ö. Farkas, J. B. Foresman, J. V. Ortiz, J. Cioslowski and D. J. Fox, *GAUSSIAN 09, Revision D.01*, Gaussian, Inc., Wallingford, CT, 2009.
- 29 Stuttgart RSC 1997 ECP basis sets used in this work and the related references therein can be obtained from <https://bse.pnl.gov/bse/portal>.
- 30 J. Cizek, *Adv. Chem. Phys.*, 1969, **14**, 35.
- 31 (a) G. E. Scuseria and H. F. Schaefer III, *J. Chem. Phys.*, 1989, **90**, 3700; (b) G. E. Scuseria, C. L. Janssen and H. F. Schaefer III, *J. Chem. Phys.*, 1988, **89**, 7382.
- 32 J. A. Pople, M. Head-Gordon and K. Raghavachari, *J. Chem. Phys.*, 1987, **87**, 5968.
- 33 (a) P. v. R. Schleyer, C. Maerker, A. Dransfeld, H. J. Jiao and N. J. R. v. E. Hommes, *J. Am. Chem. Soc.*, 1996, **118**, 6317; (b) P. v. R. Schleyer, H. J. Jiao, N. J. R. v. E. Hommes, V. G. Malkin and O. L. Malkina, *J. Am. Chem. Soc.*, 1997, **119**, 12669.
- 34 E. D. Glendening, J. K. Badenhoop, A. E. Reed, J. E. Carpenter, J. A. Bohmann, C. M. Morales and F. Weinhold, *NBO 5.0*, Theoretical Chemistry Institute, University of Wisconsin, Madison, WI, 2001.
- 35 P. Pykkö, *J. Phys. Chem. A*, 2015, **119**, 2326.
- 36 M. E. Casida, C. Jamorski, K. C. Casida and D. R. Salahub, *J. Chem. Phys.*, 1998, **108**, 4439.
- 37 R. Bauernschmitt and R. Ahlrichs, *Chem. Phys. Lett.*, 1996, **256**, 454.
- 38 T. J. Kealy and P. L. Pauson, *Nature*, 1951, **168**, 1039.
- 39 R. Zhang, Y. J. Ji, L. Yang, Y. Zhang and G. C. Kuang, *Phys. Chem. Chem. Phys.*, 2016, **18**, 9914.
- 40 Z. U. Abidin, L. Wang, H. J. Yu, M. Saleem, M. Akram, N. M. Abbasi, H. Khalia, R. L. Sun and Y. S. Chen, *New J. Chem.*, 2016, **40**, 3155.
- 41 L. Peng, A. C. Feng, M. Huo and J. Y. Yuan, *Chem. Commun.*, 2014, **50**, 13005.
- 42 Š. Toma, J. Csizmadiová, M. Mečiarová and R. Šebesta, *Dalton Trans.*, 2014, **43**, 16557.
- 43 L. Y. Zhu and J. L. Wang, *J. Phys. Chem. C*, 2009, **113**, 8767.
- 44 S. S. Mallajosyula, P. Parida and S. K. Pati, *J. Mater. Chem.*, 2009, **19**, 1761.
- 45 M. D. Su and S. Y. Chu, *J. Phys. Chem.*, 1991, **95**, 9757.
- 46 T. Wettling, G. Wolmershauser, P. Binger and M. Regitz, *J. Chem. Soc., Chem. Commun.*, 1990, **21**, 1541.
- 47 (a) T. Kurikawa, H. Takeda, M. Hirano, K. Judai, T. Arita, S. Nagao, A. Nakajima and K. Kaya, *Organometallics*, 1999, **18**, 1430; (b) A. Nakajima and K. Kaya, *J. Phys. Chem. A*, 2000, **104**, 176.